Radiated Emission from the Slot of a Slim Cubical Enclosure with Multiple Sources Inside

Christian Poschalko[(1)] and Siegfried Selberherr[(2)]

[(1)] Robert Bosch AG
Vienna, Austria, Email: christian.poschalko@at.bosch.com
[(2)] Institute for Microelectronics, Technische Universität Wien
Vienna, Austria, Email: selberherr@TUWien.ac.at

***Abstract*— An efficient analytical model for the prediction of the radiated emission from the slot of a slim cubical enclosure with multiple sources inside is developed. We use this model to obtain the far field diagrams and the radiated power at the resonance frequencies, where emission becomes dominant. The radiated power from the slot of the enclosure depends on the number of sources, on their locations, amplitudes, and phase relations, even at low frequencies below the first resonance. We present the radiated power for some cases with one and two sources inside the enclosure. The analytical formulations allow to analyze the field distribution inside the enclosure and the radiated emission, which may be used to obtain placement and layout rules for critical components.**

I. INTRODUCTION

Cavity field models are established for the full wave description of power plane fields [1], [2] and the far field radiation calculation of rectangular power planes [3], [4]. Such analytical formulations have a lot of advantages for practical applications:

- Fields can be calculated much faster than by numerical field simulation.
- Resonance frequencies can be calculated from closed form expressions.
- Positions of maximum field values can be found by discussion of the analytical expressions for a wide frequency range.
- The influence of the position of electronic components can be investigated .

Slim metallic enclosures (Fig. 1) are required for many applications, such as (CD/DVD) drives, slots for 19'' racks, shielding covers for displays or other sensitive devices, or automotive control devices.
When the distance of the cover to the bottom of such devices is small compared to the wavelength, a cavity field formulation is applicable in order to describe the fields, e.g. [1] - [6].

The field inside an enclosure with metallic walls can be calculated with these formulations by introduction of a sufficient amount of low impedance components to ports at the edges. However, the different boundaries result in changes regarding resonance frequencies and maximum field position, which cannot be investigated by simple discussions of the analytical expression, because the boundary conditions are not satisfied by the basis functions of the analytical formulation. We developed a cavity field formulation using three perfectly electric conducting walls (PEC) on the closed sides of the enclosure and one perfectly magnetic conducting boundary condition (PEM) on the open slot (Fig. 1).

Based on this cavity formulation, we obtained a closed form expression for the radiated electric far field, using the equivalent source method similarly as it has been done by [3] for planes with open boundaries. To consider the closed metallic walls of the enclosure, we use the wall currents from the cavity field formulation for the far field integration to obtain an approximate formulation for the evaluation of the far field diagrams. For the calculation of the radiated power we do not consider the wall influence, because the contribution of the walls to the radiated power is low, as we confirmed by HFSS® simulations.

The expressions for the cavity fields inside the enclosure and the electric far field are presented in Section II (Fig. 1).

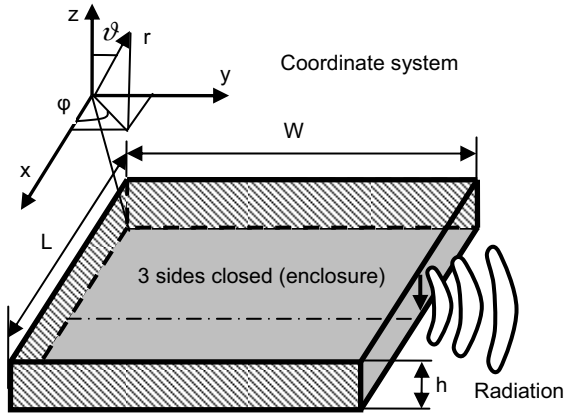

Figure 1. A cubical metallic enclosure with three closed edges and one open slot. Cover and botton are also metallic surfaces.The cavity field inside the enclosure causes radiated emission from the open slot.

For the derivation of placement and layout rules, it is necessary to know the influence of multiple sources (within the enclosure) on the radiation. [4] has shown a significant influence of multiple sources on the radiation of rectangular power planes with four open sides.

In Section III we present the radiated power for one and two sources within the enclosure in order to demonstrate that multiple sources have a significant influence on the radiated emissions from the slot of the enclosure. Our examples show that radiation modes can even be suppressed by proper source placement.

II. Cavity Model and Electric Far Field Expression for a Slim Cubical Enclosure

We derived the cavity field formulations within the enclosure depicted in Fig. 1, by using the scalar Helmholz equation (1) similarly as it has been done for rectangular planes with open boundaries by [1], [2].

$$\vec{\nabla}^2 E_z + \omega^2 \cdot \mu_0 \cdot \varepsilon_0 \cdot E_z = j \cdot \omega \cdot \mu \cdot J_z \qquad (1)$$

E_z *z component of the electric field (between the planes)*

J_z *z component of the current density*

Using the separation method and introducing PEC boundary conditions for the closed walls and a PEM boundary condition for the open slot, the solution of (1) becomes:

$$Z_{ij} = \frac{j \cdot \omega \cdot \mu_0 \cdot h}{L \cdot W} \cdot \sum_{m=0}^{\infty} \sum_{n=0}^{\infty} \left\{ \frac{4 \cdot So_{ij}}{k_{x,m}^2 + k_{y,m}^2 - k^2} \right\} \qquad (2)$$

$$So_{ij} = \sin\left(k_{x,m} \cdot x_i\right) \cdot \sin\left(k_{y,n} \cdot y_i\right) \cdot \sin\left(k_{x,m} \cdot x_j\right) \cdot \sin\left(k_{y,n} \cdot y_j\right) \qquad (3)$$

x_i, y_i, x_j, y_j *port positions of port i and j* (4)

$$k_{x,m} = \frac{m \cdot \pi}{L}, \quad k_{y,n} = \frac{(2 \cdot n + 1) \cdot \pi}{2 \cdot W}, \quad k = \frac{\omega}{c_0} \qquad (5)$$

The voltage between the upper and the lower plane at position (x_i, y_i) is given by:

$$U_i(x_i, y_i) = \sum_{j=1}^{n\_port} \left(Z_{ij}(x_i, y_i, x_j, y_j) \cdot I_j(x_j, y_j) \right) \qquad (6)$$

$I_j(x_j, y_j)$ *current on port j*

n_port *number of ports*

The electric field inside the enclosure is given by:

$$\vec{E}_i(x_i, y_i) = \frac{U_i(x_i, y_i)}{h} \cdot \vec{e}_z \qquad (7)$$

The resonance frequencies of the enclosure evaluate to:

$$f_r = \frac{c_0}{2 \cdot \pi} \cdot \sqrt{\left(\frac{m \cdot \pi}{L}\right)^2 + \left(\frac{(2 \cdot n + 1) \cdot \pi}{2 \cdot W}\right)^2} \qquad (8)$$

This shows that an enclosure with only one open slot has different resonance frequencies as two planes with four open boundaries.

Resonance frequencies of the modes with m=0 do not exist, because the nominator of (2) vanishes at the same frequency as the denominator. For example, an enclosure with *L=160mm* and *W=120mm* has the resonance frequencies summarized in Table I:

TABLE I.
Resonance Frequencies of an Enclosure with One Open Edge

Mode		Resonance frequency	Exist
m	**n**	**MHz**	**yes/no**
0	0	625	no
1	0	1127	yes
0	1	1875	no
1	1	2096	yes

Table II contains the resonance frequencies of two planes with *L=160mm, W=120mm* and four open edges, which were calculated following [1]:

$$f_r = \frac{c_0}{2 \cdot \pi} \cdot \sqrt{\left(\frac{m \cdot \pi}{L}\right)^2 + \left(\frac{n \cdot \pi}{W}\right)^2} \qquad (9)$$

TABLE II.
Resonance Frequencies of an Enclosure with Four Open Edges

Mode		Resonance frequency	Exist
m	**n**	**MHz**	**yes/no**
0	0	-	no
1	0	938	yes
0	1	1250	yes
1	1	1563	yes

Table I and Table II show that the resonance frequencies of the cavity field depend significantly on the boundary conditions. Equation (8) offers a quick opportunity to estimate the resonance frequencies of a slim enclosure.

Expression (3) shows directly that the maximum values of the field will be at the slot and also that the placement of a single source near to the enclosure walls will reduce the emission of this source.

With (7) for the electric fields at the slot of the enclosure, we obtain the electric far field applying equivalent source theory:

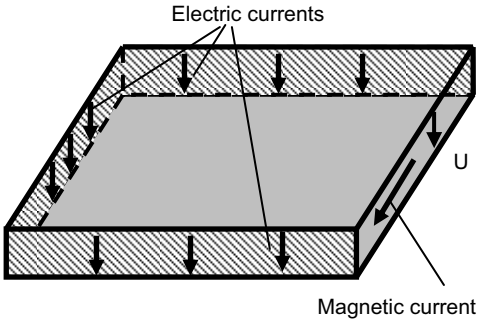

Figure 2. Magnetic currents on the slot, calculated from the slot voltage distribution (2) and electric currents on the walls to consider the influence of the enclosure approximately.

The magnetic currents $\vec{M}$ are related to the voltage U at the slot by:

$$\vec{M} = \vec{E} \times \vec{n} = U / h \cdot \vec{e}_x \tag{10}$$

$\vec{n}$ *unit vector normal to enclosure walls*

To obtain the expression for the electric far field contribution from the slot we integrate (10) [3], [7]:

$$\vec{E} = \frac{j \cdot k}{4 \cdot \pi} \cdot \frac{e^{-j \cdot k \cdot r}}{r} \cdot h \cdot \oint_{\zeta} \left\{ \vec{M} \cdot e^{j \cdot k \cdot \vec{r}\,' \cdot \vec{e}_r} \cdot (\vec{e}_r \times \vec{e}_l) \cdot dl' \right\} \tag{11}$$

r' is the vector from the origin of the coordinate system Fig. 1 to the source location at the slot.

$\vec{e}_l$ *unit vector* tan *gential to the* int *egration line*

The expression for the electric far field contribution from the slot is given by:

$$\vec{E}_{sl} \approx -\frac{k \cdot \omega \cdot \mu_0 \cdot h}{\pi} \cdot \vec{R}_{sl} \cdot \frac{e^{-j \cdot k \cdot r}}{r} \cdot \sum_{m=0}^{\infty} \sum_{n=0}^{\infty} \left(A_{mn} \cdot (-1)^n \cdot e^{j \cdot k_\eta \cdot W} \cdot R_l \right) \tag{12}$$

$$\vec{R}_{sl} = \sin(\varphi) \cdot \vec{e}_\vartheta + \cos(\varphi) \cdot \cos(\vartheta) \cdot \vec{e}_\varphi \tag{13}$$

$$Amn = \frac{I_s}{L \cdot W} \cdot \frac{\sin(k_m \cdot x_S) \cdot \sin(k_n \cdot y_S)}{\left(k_m^2 + k_n^2 - k^2\right)} \tag{14}$$

$$R_l = \frac{k_m}{k_m^2 - k_\xi^{\,2}} \cdot \left(1 - (-1)^m \cdot e^{j \cdot k_\xi \cdot L}\right) \tag{15}$$

$$\begin{pmatrix} k_\xi \\ k_\eta \end{pmatrix} = k \cdot \sin(\vartheta) \cdot \begin{pmatrix} \cos(\varphi) \\ \sin(\varphi) \end{pmatrix} \tag{16}$$

x_s, y_s and I_s are the source parameter.

The far field pointing vector is given by:

$$\vec{S} = \frac{k}{\omega \cdot \mu} \cdot \left|\vec{E}\right|^2 \cdot \vec{e}_r \tag{17}$$

For the calculation of the radiated power we used expressions (11) – (17) and did not consider the influence of the walls. Therefore the main contribution to the radiated power comes from the slot fields. However, the walls have an influence on the radiation diagrams. To consider this influence, we used the cavity field formulation (7), (18) to calculate the currents $\vec{J}$ on the internal walls of the enclosure. We approximated the currents on the external walls by these internal current formulations and integrated these currents for the far fields using (18) and (19):

$$\vec{J} = \vec{n} \times \vec{H} \tag{18}$$

$$\vec{H} = -\frac{j \cdot k}{4 \cdot \pi} \cdot \frac{e^{-j \cdot k \cdot r}}{r} \cdot h \cdot \oint_{\zeta} \left\{ \vec{J} \cdot e^{j \cdot k \cdot \vec{r}\,' \cdot \vec{e}_r} \cdot (\vec{e}_r \times \vec{e}_l) \cdot dl' \right\} \tag{19}$$

$$\vec{E} = 1/(j \cdot \omega \cdot \varepsilon_0) \cdot (\vec{\nabla} \times \vec{H}) \quad (20)$$

The formulation of the external currents by the internal solution (7) is an approximation, where comparisons with HFSS® simulations showed a good agreement. Therefore, the approximation can be used to get first order information about the radiation diagrams, much faster than by simulation.

The following expressions have been obtained to approximate the far field contribution from the enclosure walls. The contribution of the back wall is given by (21):

$$\vec{E}_{bw} \approx -\frac{0.1 \cdot \omega \cdot \mu_0 \cdot h}{\pi} \cdot \sin(\vartheta) \cdot \vec{e}_\vartheta \cdot \frac{e^{-j \cdot k \cdot r}}{r} \cdot \sum_{m=0}^{\infty} \sum_{n=0}^{\infty} (A_{mn} \cdot k_n \cdot R_l) \quad (21)$$

The contribution of the side walls are approximated by (22):

$$\vec{E}_{sw} \approx -\frac{0.1 \cdot \omega \cdot \mu_0 \cdot h}{\pi} \cdot \sin(\vartheta) \cdot \frac{e^{-j \cdot k \cdot r}}{r} \cdot \vec{e}_\vartheta \cdot \sum_{m=0}^{\infty} \sum_{n=0}^{\infty} \left(A_{mn} \cdot k_m \cdot m \cdot R_w \cdot \left(1 - (-1)^m \cdot e^{j \cdot k_\xi \cdot L}\right)\right) \quad (22)$$

With:

$$R_w = \frac{j \cdot k_\eta}{k_n^2 - k_\eta^2} \cdot (-1)^n \cdot e^{j \cdot k \eta \cdot W} + \frac{k_n}{k_n^2 - k_\eta^2} \quad (23)$$

The radiated field is given by the summation of (12), (21) and (22):

$$\vec{E}_F \approx \vec{E}_{sl} + \vec{E}_{bw} + \vec{E}_{sw} \quad (24)$$

As (12) is a linear function of the source current, the electric far field power of multiple sources can be calculated by a simple superposition of the fields from each individual source. The influence of every source can, therefore, be investigated individually by (12). The radiated power has to be calculated from the superposed electric field (17). We use (12)-(24) in Section III to obtain the radiation diagrams of the first modes.

Expression (2) does not consider any losses. Therefore, the fields inside the enclosure described by (2) will deviate to the real lossy situation, especially at the resonance frequencies. Power planes have a very small plane separation (h in Fig.1) and, therefore, the radiation loss can be neglected compared with the dielectric loss of the substrate and the conduction loss [3], [4]. In case of an enclosure the plane separation is much higher and radiation becomes the dominant loss mechanism [4] [5] [6], because the radiated power is proportional to h^2 (16) (17).

As the enclosure is filled up by air, the dielectric losses are small as are the conducting losses, because the currents are significantly smaller than in the case of power planes.

The radiation loss can be considered in the cavity field calculation by a quality factor which can be obtained by applying the method of [5]. (2) and (7) are used together with an effective wave number which introduces the radiation loss:

$$E_z(x_i, y_i) = \frac{j \cdot \omega \cdot \mu_0}{L \cdot W} \cdot I_j \cdot \sum_{m=0}^{\infty} \sum_{n=0}^{\infty} \left\{ \frac{4 \cdot So_{ij}}{k_{x,m}^2 + k_{y,m}^2 - k_{eff}^2} \right\} \quad (25)$$

With:

$$k_{eff} = \frac{\omega}{c_l} \cdot \left(1 - j \cdot \frac{1}{2 \cdot Q_r}\right)$$
$$Q_r \ldots quality\ factor\ for\ radiation\ loss\ consideration \quad (26)$$

According to [5], the Quality factor *Qr* can be obtained by:

$$Q_r = \omega \cdot \frac{U_s}{P_r} \quad (27)$$

Us is the stored energy in the cavity volume given by:

$$U_s = 2 \cdot \iiint_V \left(\frac{1}{4} \cdot \varepsilon_0 \cdot \left|\vec{E}\right| \right) \cdot dV \quad (28)$$

Pr is the radiated power given by:

$$P_r = \frac{1}{2} \cdot \int_{\varphi=0}^{2 \cdot \pi} \int_{\vartheta=0}^{\pi} \left|\vec{S}\right| \cdot r^2 \cdot \sin(\vartheta) \cdot d\vartheta \cdot d\varphi \quad (29)$$

Radiation loss is dominant at the resonance frequencies. Therefore it is sufficient to calculate *Qr* only for the resonance frequencies. The introduction of the loss factor *Qr* is necessary to obtain correct fields inside the enclosure. However, *Qr* needs not to be

considered for the calculation of the radiation diagrams, as it does not change the geometrical field distribution.

III. RADIATION DIAGRAMS AND RADIATED POWER

Figure 3 shows the radiation diagrams for the first six modes in case of a source at position x_S=L/3, y_S=W/3.

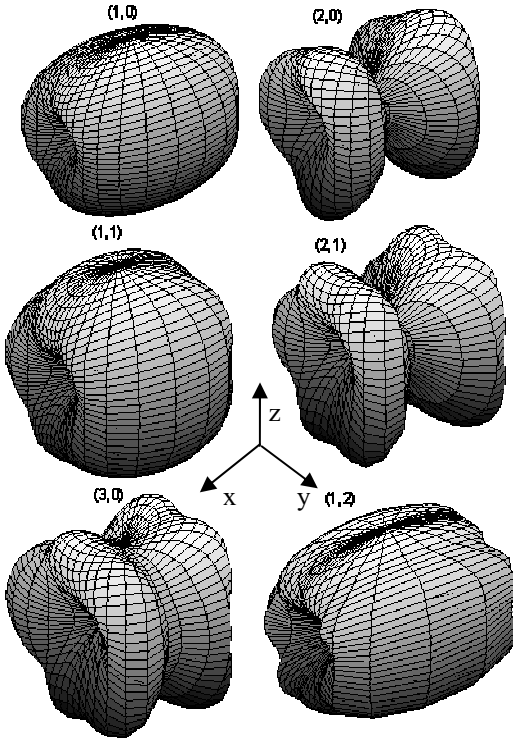

Figure 3. Radiation diagrams of a slim cubical enclosure, with a source at x=L/3 and y=W/3 corresponding to the Coordinate system in Fig. 1. for the first six modes.

The radiation diagrams show that the positions of the field maxima vary over the sphere.

We use (12) and (17) to calculate the radiated power for different sources and source positions, to show the influence of source placement on the radiated emission.

As a first example, we compare the radiated power, when one of two sources inside an enclosure is relocated. The currents of the two sources are I1=I and I1=-I. This is a relevant case, as an IC driver output will excite the planes with a phase shift to the excitation from the IC input, to which the driver output is connected by some interconnects. A field scan above a printed circuit board shows this, when high field quantities are measured above the output IC pin and the input IC pin.

Figure 4 shows that the first resonance frequency can be suppressed by the source placement, because this mode vanishes, when the source associated terms in (12) are superposed for the two source currents I and –I. The radiated power changes not only at this resonance frequency. It is reduced from low frequencies up to nearly the second resonance. Therefore the radiated emission of a device with a slotted enclosure can be significantly reduced by correct source placement.

It will not be possible to place every trace and IC on a real printed circuit board at the best location for emission reduction. However, EMC designers should concentrate on the critical signals, such as clock traces. These can be evaluated by the expressions (7) , (12), and (17).

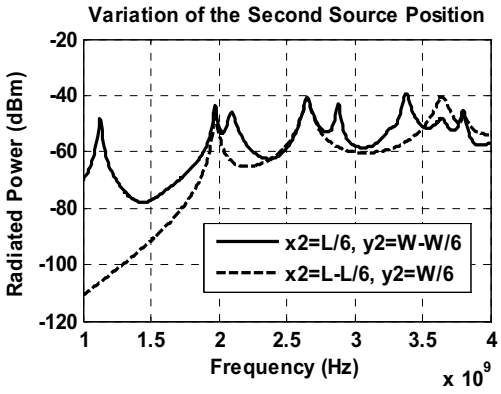

Figure 4. Comparison of the radiated power by the variation of the source position of the second source. The position of the first source is x1=L/6 and y1=W/6 in both cases.

The radiated emission initiated by a single source can be significantly reduced, when the source is moved closer to the wall of the enclosure. As an example we present the radiated power of an enclosure with L=160mm, W=120mm and h=7mm and varying source positions (Fig. 5):

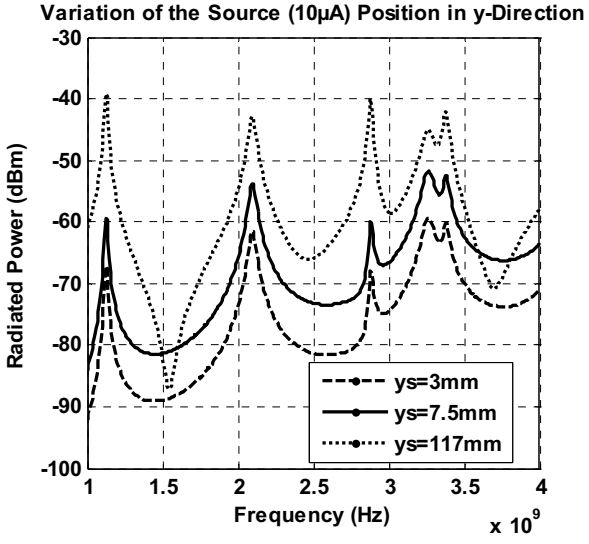

Figure 5. Variation of the excitation source position (xs=80mm).The radiated power decreases, when the source is placed near the rear wall. The coordinates (x_s, y_s) correspond to the Coordinate system in Fig. 1.

This is consistent to the fact that (3) vanishes at the metallic walls. Any move of a single source closer to the walls reduces the emission, however the reduction is dominant close to walls, where the variation of (3) has a maximum. In case of two sources with same current amplitudes but a phase relation of π, a reduction cannot generally be achieved by a move of these sources closer to the enclosure walls. When these sources are placed close to each other, the variation of (3) will get dominant for the radiation, because in case of a vanishing variation of (3), the superposition of the fields will nearly vanish too. The variation of (3) vanishes at the slot and as Fig. 6 and Fig 7 show, the radiated fields are reduced for some frequency ranges, when the two sources are moved close to the middle of the slot.

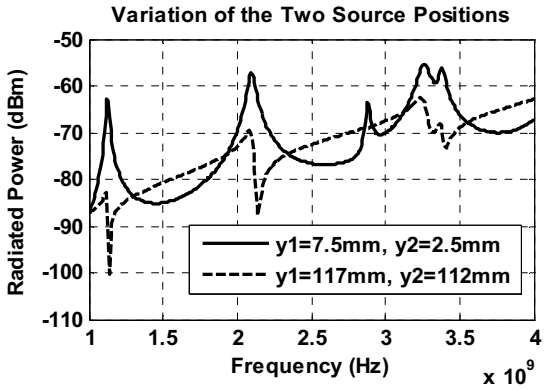

Figure 6. Variation of the excitation source positions for a source with a current nearby currents with the same amplitude, but a phase shift of π. All source positions correspond to the Coordinate system in Fig. 1. The values x1=x2=L/2 are 80mm in both cases.

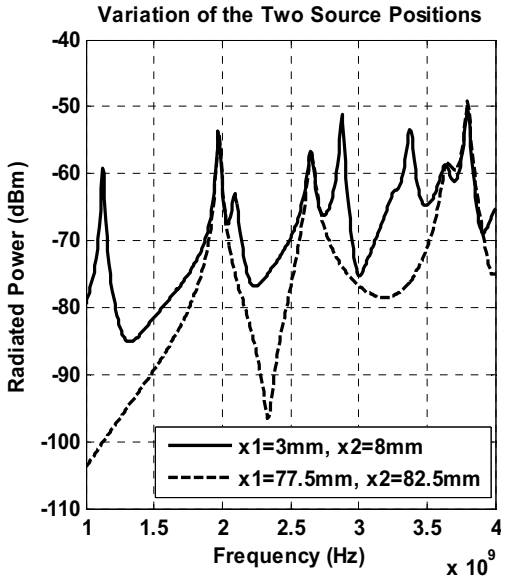

Figure 7. Variation of the excitation source positions for a source with a current nearby currents with the same amplitude, but a phase shift of π. All source positions corresponding to the Coordinate system in Fig. 1. The values y1=y2=W-3mm are 117mm in both cases.

The cases presented in Fig. 6 and Fig. 7 are extreme, because the two current sources are very close to each other. In addition, they have been moved along the edge of the enclosure, which gives a different behaviour of such sources, compared with single sources. This result should be considered for placement and layout design purposes.

IV. CONCLUSIONS

Closed form expressions have been presented for the cavity fields within a slim, cubical, metallic enclosure with three closed walls and a slot on one side. We also presented an analytical formulation for the far fields.

We presented how to use the expressions for the calculation of the radiated power.

These expressions offer an efficient method for the investigation of the contribution of source placement on the radiated emission of a cubical enclosure. This efficiency is necessary in case of a complex PCB with numerous sources inside of the enclosure. The bottom of the enclosure in Fig. 1 might be the ground plane of such a PCB, which is connected to the closed enclosure walls.

We illustrated the significance of a proper source placement for the radiated emission of a device.

ACKNOWLEDGMENT

This work was supported by the Medea+ Parachute program.

REFERENCES

[1] G.-T. Lei, R. W. Techentin, and B. K. Gilbert, "High-Frequency Characterization of Power/Ground-Plane Structures", IEEE Trans. Microw. Theory Tech., Vol. 47 No. 5, May 1999, pp.562-569

[2] C. Wang, J. Mao, G. Selli, S. Luan, L. Zhang, J. Fan, D. J. Pommerenke, R. E. DuBroff, J. L. Drewniak, "An Efficient Approach for Power Delivery Network Design with Closed-Form Expressions for Parasitic Interconnect Inductances", IEEE Trans. of Adv. Packaging, Vol.29, No.2, May 2006, pp.320-334

[3] Marco Leone, "The Radiation of a Rectangular Power-Bus Structure at Multiple Cavity-Mode Resonances", IEEE Trans. on Electromagnetic Compatibility, Vol. 45, No.3, August 2003, pp.486-492

[4] Hwan-Woo Shim, Todd H. Hubing, "A Closed-Form Expression for Estimating Radiated Emissions From the Power Planes in a Populated Printed Circuit Board", IEEE Trans. on Electromagnetic Compatibility, Vol.48, No. 1, February 2006, pp. 74-81

[5] Richard L. Chen, Ji Chen, Todd H. Hubing, Weimin Shi, "Via Coupling within Power-Return Plane Structures Considering the Radiation Loss", International Symposium on Electromagnetic Compatibility 2004, EMC 2004, Vol.2, August 2004, pp.386-391

[6] Richard L. Chen, Ji Chen, Todd H. Hubing, Weimin Shi, "Analytical Model for the Ractangular Power-Ground Structure Including Radiation Loss.", IEEE Trans. on Electromagnetic Compatibility, Vol. 47, No. 1, February 2005, pp. 10-16

[7] W. L. Stutzmann and G. A. Thiele, Antenna Theory and Design. New York: Wiley, 1981